Calculation of Coherent Synchrotron Radiation in the TTF-FEL Bunch Compressor Magnet Chicanes

M.Dohlus, T. Limberg

Deutsches Elektronen Synchrotron, Notkestr. 85, 22607 Hamburg, Germany

Abstract

The bunch compression system in the TTF-FEL decreases the bunch length in order to achieve the high peak currents needed for the SASE FEL process. Along the curved trajectories in the bunch compressor magnet chicanes, these short bunches will start to radiate coherently. In this paper, a numerical calculation of the characteristics of this radiation is presented. One-dimensional bunch models are not sufficient for near field effects in particular cannot completely explain the power flow to the EM field, but they can be used to estimate the radiation in the far region. For the calculation of the power flow, in presence of shielding by horizontal conducting planes, and of the far-field, a two-dimensional bunch with time dependent shape was simulated.

1 Introduction

A bunch of ultra-relativistic charged particles radiates incoherent as well as coherent synchrotron light. The incoherent radiation is calculated using a point particle model, leading to the radiated power

$$P_i = \frac{1}{6\pi}\frac{e^2 c_0}{\varepsilon_0}\frac{N\gamma^4}{R_0^2}$$

with N the number of particles, γ the relativistic factor and R_0 the bending radius. As the typical wavelength is of the order of the 'critical wavelength' $\lambda_c = \frac{4\pi}{3}\frac{R_0}{\gamma^3}$, which is usually small compared to the dimensions of the structure and even to the mean particle distance, this radiation is independent of the shape of the vacuum chamber and bunch. In contrast to this, the spectral components with wavelength of the order of the bunch dimensions have to be calculated from a continuous model (e.g.[1, 2]). Although the bunch length needed for FEL applications is significantly smaller than the beam pipe dimensions, the interaction length due to the retarded position of source particles is typically of the order of $L_o = \sqrt[3]{24R_0^2\sigma}$ (with the RMS bunch length σ) and therefore usually not small compared to the chamber size.

In section 2 the coherently radiated synchrotron light power is calculated for bunches in circular motion (CM-case) and the power transfer to the EM field for a TESLA bunch

compressor III design (BC-case). In both cases the effect of shielding by horizontal perfectly electric conducting (PEC) planes is investigated. For the CM-case with a rigid one-dimensional bunch, compact expressions for the radiated power and its spectrum can be formulated, in which only the shielding functions have to be integrated numerically. The BC-case is much more complex as the essentially two-dimensional charge distribution changes its shape over the hole length of the device. Therefore the E-field in the compressor is integrated numerically for a set of sub-bunches with individual paths.

In the section 3 the electrical far-field in forward direction is derived and time signals as well as spectra are calculated for the BC-case, using the sub-bunch approach.

2 Power Flow to the EM Field

The electrical field $\vec{E}(\vec{r},t)$ of a charge distribution $\rho(\vec{r},t)$ with a given motion $\vec{v}(\vec{r},t)$ can be calculated directly from the retarded potential approach:

$$\vec{E}(\vec{r},t) = -\nabla V - \dot{\vec{A}} = -\nabla \frac{1}{4\pi\varepsilon} \int \frac{\rho(\vec{r}',t')}{\|\vec{r}-\vec{r}'\|} dV' - \frac{\mu}{4\pi} \int \frac{\dot{\rho}(\vec{r}',t')\vec{v}(\vec{r}',t')}{\|\vec{r}-\vec{r}'\|} dV' \ . \tag{1}$$

This integration can be simplified for the case of a rigid one-dimensional bunch with the charge density $\lambda(s,t) = \lambda(s-\beta ct)$, traveling on a general path $\vec{r}_s(s)$:

$$\vec{E}(\vec{r},t) = \frac{1}{4\pi\varepsilon_0} \int \left\{ \frac{\beta\lambda'}{R} \left(\beta\vec{e} - \vec{n}\right) + \frac{\lambda}{R^2}\vec{n} \right\} ds \tag{2}$$

with $\vec{R} = \vec{r} - \vec{r}_s(s)$, $\vec{n} = \vec{R}/R$, $\vec{e} = \partial\vec{r}_s(s)/\partial s$ and $\lambda = \lambda(s+\beta(R-c_0t))$. To avoid the singularity of the kernel, the field is split into $\vec{E}_2 = \vec{E}\left\{\text{path} = \vec{r}_s(s_0) + (s-s_0)\vec{e}(s_0)\right\}$ and $\vec{E}_1 = \vec{E}\left\{\text{path} = \vec{r}_s(s)\right\} - \vec{E}_2$. The reference point $\vec{r}_s(s_0)$ is the point of the path which is closest to the observation point. The field $\vec{E}_1$ is integrated numerically while an analytical expression is used for $\vec{E}_2$.

According to Maxwell's equations the total change of electro-magnetic field energy is

$$\frac{d}{dt} W_{\text{field}} = P(t) = -\int \vec{E}(\vec{r},t) \cdot \vec{J}(\vec{r},t)\, dV \ . \tag{3}$$

This includes 'synchrotron light radiation' as well as the change of energy of the field which guides the beam. With the longitudinal electrical field $E(u,t) = \vec{E}(\vec{r}_s(u),t) \cdot \vec{e}(u)$ the power flow caused by an one-dimensional beam can be written as

$$P(t) = -\beta c_0 \int E(u,t)\lambda(u-\beta c_0 t) du \ . \tag{4}$$

2.1 Circular Motion

As the electrical field guiding a rigid one-dimensional bunch in circular motion is stationary, all power $P(t) =: P_c$ is radiated into the far range. The effect of horizontal PEC planes at $z = \pm h/2$ is taken into account by mirror charges $(-1)^\nu\lambda$ at $z = \nu h$. The coherently radiated power is:

$$P_c = \frac{\Gamma(5/6)}{4\pi^{3/2}\sqrt[3]{6}} \frac{e^2 c_0}{\varepsilon_0} \frac{N^2}{R_0^{2/3}\sigma^{4/3}} \cdot S_1\left(\frac{h}{\sqrt[3]{R_0\sigma^2}}\right) \ , \tag{5}$$

with the shielding function

$$S_1(x) = 1 - \frac{\sqrt[3]{6}}{4\Gamma(5/6)} \sum_{\nu=1}^{\infty} (-1)^\nu (\nu x)^{5/2} \int_{-\infty}^{0} e^{-\frac{(\nu x)^3}{4}\left(\frac{s^3}{24}-\frac{1}{2s}\right)} \left(\frac{s^4}{24} - \frac{1}{2}\right) ds \qquad (6)$$

as plotted in Fig.1. The essential approximations to derive this formula are: $\sigma \gg \lambda_c$, $\beta \to 1$ and $\lambda(s + R - c_0 t) \simeq \lambda((s-u)^3/24R_0^2 - \nu h/2(s-u) - c_0 t)$ for $s < u$. The same approach leads to the spectral power density

$$p_c(\omega) \propto \sqrt[3]{\omega}\, \mathcal{F}\{\lambda(c_0 t)\}^2 \cdot S_2\left(h \sqrt[3]{\frac{\omega^2}{c_0^2 R_0}}\right) \qquad (7)$$

with the spectral shielding function

$$S_2(x) = 1 - \frac{1}{\sqrt[6]{3}\Gamma(2/3)} \sum_{\nu=1}^{\infty} (-1)^\nu \nu x \int_{-\infty}^{0} \sin\left((\nu x)^{3/2}\left(\frac{s^3}{24} - \frac{1}{2s}\right)\right) s ds \ , \qquad (8)$$

which is also plotted in Fig.1.

For the end of the TESLA bunch compressor III design (see Tab. 1 where $\sigma = 50\mu$m and $R_0 = 29.233$m) the following values can be calculated: The incoherent radiated power P_i is 0.35W while 54 kW are radiated coherently (P_c). A shielding with horizontal planes $h = 10$mm apart, reduces this radiation to $P_c = 23.3$kW. The half of this power is radiated in the frequency range between 0.81THz and 1.24THz with the maximal spectral density at 0.96 THz.

2.2 TESLA Bunch Compressor III

A third stage of the bunch compression system for the TESLA FEL is composed of a chicane of four magnets with parameters as listed in Tab. 1. Fig. 2 plots the bunch lengths projected in the direction of motion σ_{long} and in the perpendicular direction σ_{trans} along the compressor. For a simulation of the compression process, the bunch has to be synthesized by a set of sub-bunches with the length σ_{sub}, each with a different longitudinal offset at the entrance of the compressor, a different energy and a different path. This approach leads to the two-dimensional charge distribution sketched in Fig. 2. As the field energy of a flat beam in linear motion (with the velocity of light) is

$$W_{\text{linear}} = \frac{q_0}{4\pi^{3/2}\varepsilon_0 \sigma_{\text{ls}}} \ln\left(\frac{\sigma_{\text{ls}}\, C}{\sigma_{\text{sub}}\sigma_{\text{trans}}}\right) \qquad (9)$$

with $\sigma_{\text{ls}} = \sqrt{\sigma_{\text{long}}^2 + \sigma_{\text{sub}}^2}$ and C is dependent on the geometry of the beam pipe, the conversion of a 1D to a 2D beam would lead to an infinite loss of field energy (or gain of kinetic energy). To avoid this unphysical behavior of the model, the longitudinal field is observed at a vertical offset of 20μm which corresponds approximately to a transversal width $\sqrt{2/\pi}20\mu\text{m} \simeq 16\mu$m of the sub-bunches (for more details see [1]). The result of a simulation with 500 sub-bunches ($\sigma_{\text{sub}} = 16.7\mu$m) is shown in Fig.3. It has been verified, that the calculated power exchange *in* the compressor (1m$< s <$19m) is insensitive to the parameters of the sub-bunches, but of course the effects at the entrance and exit depend strongly on the transverse dimensions of the bunch before and after compression.

To demonstrate the invalidity of a one-dimensional approach, the power exchange of a single line bunch with the local length as given by Fig.2 is shown as a dashed curve in Fig.3. Especially at the end of the third magnet the $\sigma_{\mathrm{long}}(s)$-model underestimates the power transfer. The agreement at the end of the fourth magnet is good because the bunch length is approximately constant and the transverse beam dimensions are defined by the width of the sub-bunches. The small deviation is caused by the slightly longer bunch length $\sqrt{\sigma_{\mathrm{long}}^2+\sigma_{\mathrm{sub}}^2}$ of the sub-bunch approach. For the drift spaces, the difference between the one and two-dimensional models can partially be explained by the power flow to space charge fields: $P_s = \partial W_{\mathrm{linear}}/\partial\sigma_{\mathrm{trans}} \cdot \partial\sigma_{\mathrm{trans}}/\partial t$. This formula is valid for an adiabatic transverse compression. As the particle motion in the drift spaces is linear, the field contribution $\vec{E}_2$ describes all effects with exception of the interaction with fields which have been radiated in the arcs. Therefore P_s can also be evaluated by $\int \vec{E}_2 \cdot \vec{J} dV$ which is plotted as a dotted curve in Fig.3.

For the second half of the compressor, the shielding effect of horizontal PEC planes with a separation of h is investigated. Even with shielding, the transfer of kinetic energy to field energy is maximal at the end of the third magnet where the ratio $\sigma_{\mathrm{trans}}/\sigma_{\mathrm{long}}$ is extreme (see the + curve in Fig.3 and Fig.4). The shielding in the middle of the third drift space seems to be very efficient but this is caused by local interference. At the end of drift space the power flow is approximately P_s which is needed for the energy stored in the near fields. At the beginning of the last magnet a strong oscillation appears until the steady state value is reached as estimated in section 2.1.

3 Far-field Radiation

The far-field radiation to the point $\vec{r}_f = \vec{r}_s(s_0) + X\vec{e}(s_0)$ of a one-dimensional bunch passing the point $\vec{r}_s(s_0)$ is calculated based on the assumption $\vec{n}(s) = \vec{n}(s_0) + O((\delta s/X)^2) \simeq \vec{n}(s_0) =: \vec{n}_0$ for $s_1 \le s \le s_2$. The interval $[s_1, s_2]$ is the location of the retarded bunch. Therefore the field component $E_t = \vec{E} \cdot \vec{e}_t$, perpendicular to the observer-source direction $\vec{n}$, is given by

$$E_t = \frac{1}{4\pi\varepsilon_0} \int R^{-1} \lambda' \sin(\varphi) ds \ , \tag{10}$$

with $\sin(\varphi) = \vec{e}(s) \cdot \vec{e}_t$ and $\beta \to 1$. The factor R^{-1} can be taken as $const = X^{-1}$ only for $s_2 - s_1 \ll X$. Nevertheless this approximation allows a qualitative estimate, even when this condition is not fully satisfied e.g. if X is of the order of few meters. Eqn. (10) is most sensitive to the approximation used in the argument of the line charge density:

$$\lambda' = \lambda' \left(s_0 + X - c_0 t + \frac{1}{2} \int_{s_0}^{s} \varphi(\eta)^2 d\eta \right) \ . \tag{11}$$

A typical property of the far-field is its insensitivity to offsets perpendicular to the source-observer direction, so that only longitudinal properties of the beam ($\propto \sigma_{\mathrm{long}}$ see Fig.2) can be detected! To get more information of the compression process in TESLA BC3, one can either compare the radiation from different positions along the chicane or vary the initial energy spread. The time functions and spectra in Fig.5 are calculated by the sub-bunch approach without further simplifications. The radiation in the direction of the drift spaces, caused by the arcs before and behind, is seen as single pulse (curve a and c).

In other directions (e.g. tangential to the 13m position, see curve b) the radiation can be distinguished in time. According to this, the spectrum (curve d) has a strong modulation.

4 Summary

The power flow to the EM field and the far-field radiation of a two-dimensional bunch with time dependent profile has been calculated for a third stage of the TESLA FEL bunch compressor. One-dimensional bunch models are not sufficient to describe near fields, the power flow and the shielding effect by horizontal PEC planes. This has been demonstrated by two examples: 1D bunch in circular motion, 1D bunch in BC3 with local length $\sigma_{\mathrm{long}}(s)$. Especially in the drift spaces, where the bunch changes only its transverse dimensions, a significant contribution of the power exchange is needed for the near field which guides the beam. In contrast to this, the far-field observed in the longitudinal direction is insensitive to transverse bunch dimensions.

References

[1] M.Dohlus, T.Limberg: 'Emittance Growth due to Wake Fields on Curved Bunch Trajectories', FEL Conference, Rome, August 1996, to be published in Particle Accelerators.

[2] M.Dohlus, A.Kabel, T.Limberg: 'Wake Fields of a Bunch on a General Trajectory Due to Coherent Synchrotron Radiation', Particle Accelerator Conference, Vancouver, May 1997.

bunch charge	C	10^{-9}	magnet length	m	3
compression	μm	$250 \rightarrow 50$	deflection angle	deg	5.88
energy	MeV	516	length of drift space 1 & 3	m	3
linear energy spread	$\delta E/E$	0.001893	length of drift space 2	m	2

Table 1: Parameters of a design for the third stage of the TESLA FEL bunch compression system.

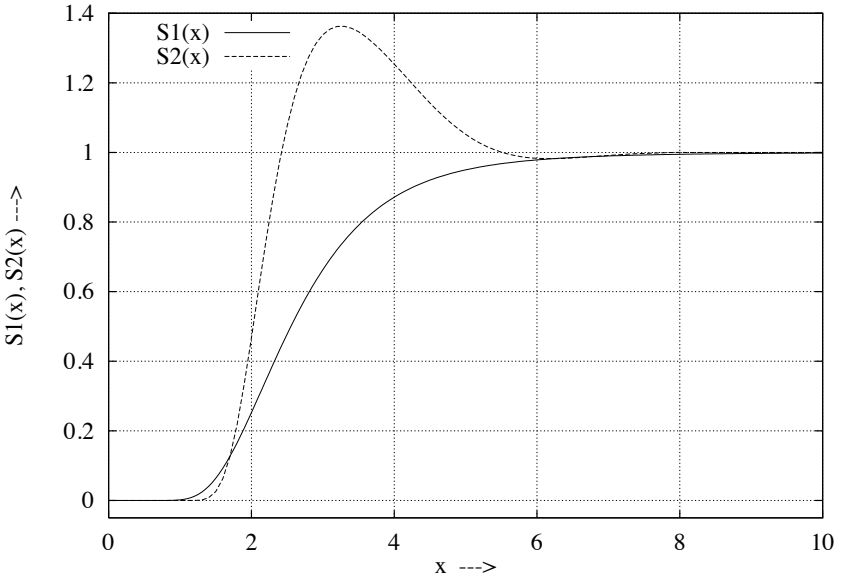

Figure 1: Shielding functions $S_1\Big(x = h/\sqrt[3]{R_0\sigma^2}\Big)$ and $S_2\Big(x = h\sqrt[3]{\omega^2/(c_0^2 R_0)}\Big)$.

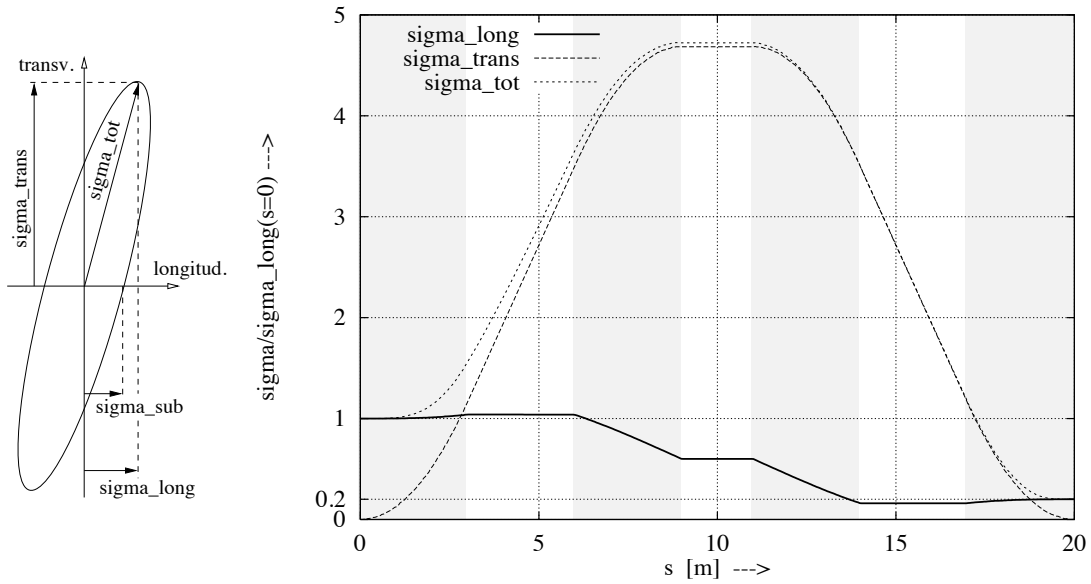

Figure 2: Bunch dimensions in TESLA bunch compressor III. The ranges in the magnets are shaded.

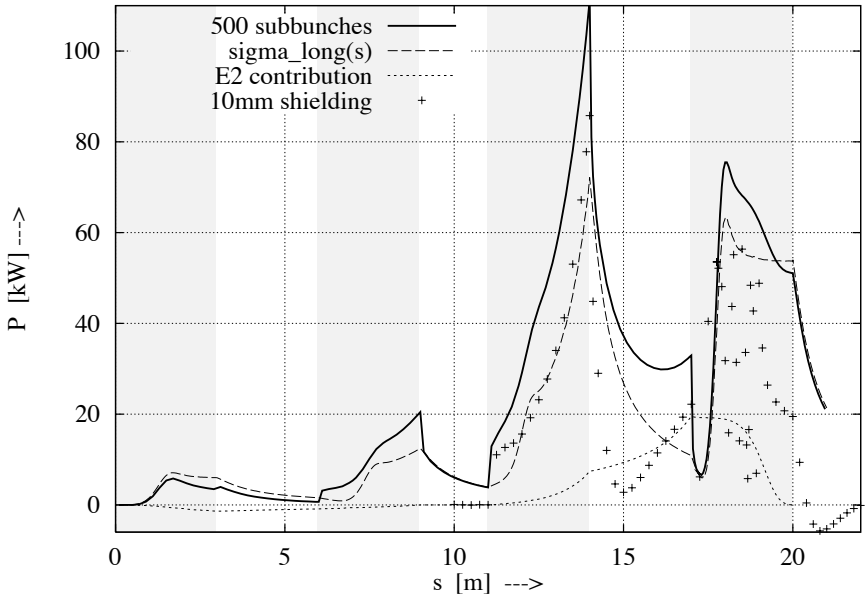

Figure 3: Power flow to the electromagetic field energy vs. bunch position. The shielding is calculated for s =10..20m. The ranges in the magnets are shaded.

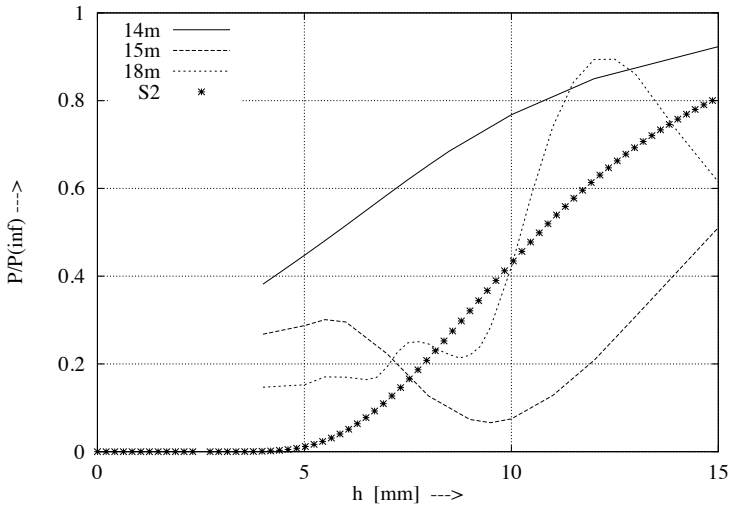

Figure 4: Shielding factor $P(h)/P(\infty)$ at different positions in the compressor and shielding function $S1$ with parameters at the end of BC3.

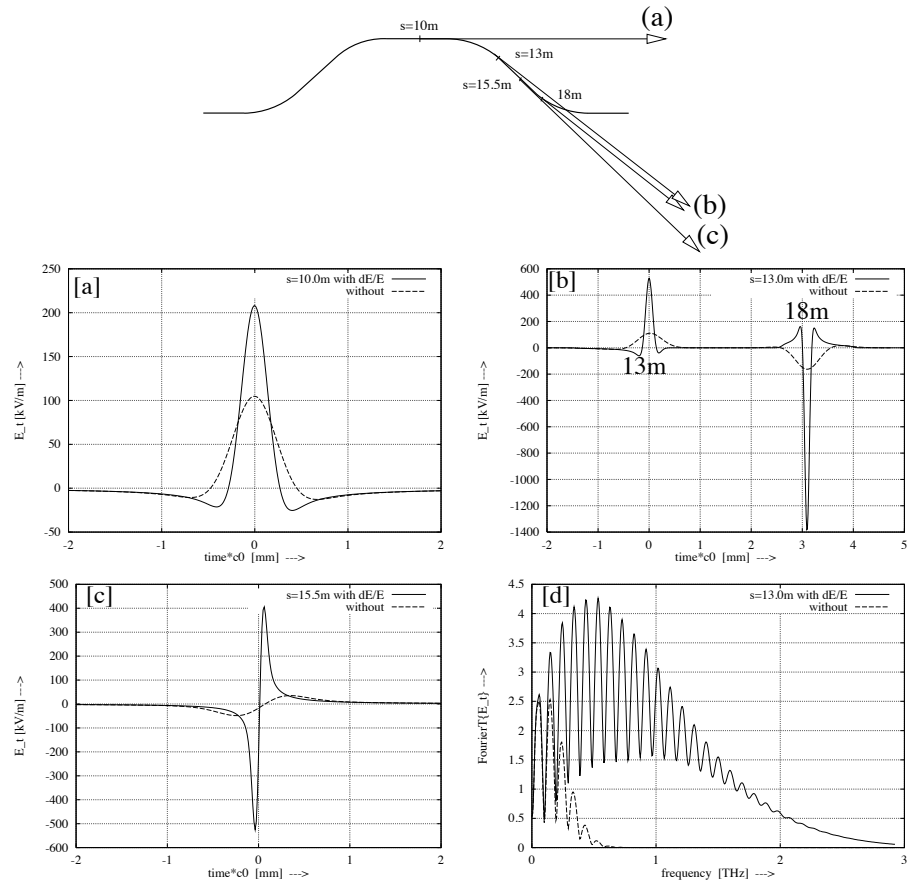

Figure 5: Transverse E-field in the far field region radiated at different locations along the bunch compressor with and without compression (energy spread $\delta E/E$). Oberservation after 15m in tangential direction: (a) $s_0 = 10$m, (b) $s_0 = 13$m and a second pulse radiated at 18m, (c) $s_0 = 15.5$m. (d) Fourier spectra of time signals (b).